J. Biomed. Eng. Res.
Vol. 25, No. 2, 97-102, 2004

소 동물 촬영을 위한 Micro-CT의 개발

이상철[1], 김호경[2], 전인곤[1], 조명혜[1], 조민형[1], 이수열[1]

[1]경희대학교 동서의학대학원 의료공학전공, [2]부산대학교 기계공학부 지능기계공학과
(2004년 2월 18일 접수, 2004년 4월 10일)

Development of a Micro-CT System for Small Animal Imaging

Sang Chul Lee[1], Ho Kyung Kim[2], In Kon Chun[1], Myung Hye Cho[1],
Min Hyoung Cho[1] and Soo Yeol Lee[1]

[1]Graduate School of East-West Medical Science, Kyung Hee University, Korea
[2]School of Mechanical Engineering, Pusan National University, Korea
(Received February 18, 2004. Accepted April 10, 2004)

요 약 : 소 동물 촬영에 이용될 수 있는 고해상도의 x-선 cone-beam micro computed tomography (micro-CT) 시스템을 개발하였다. Micro-CT 시스템은 120×120 mm2 의 2차원 평판 x-선 감지기, micro-focus x-선 발생장치, 주사 기구부, 병렬처리 영상 재구성 시스템으로 이루어져 있다. 개발된 시스템의 성능을 평가하기 위해 대조도와 공간해상도를 측정하였다. 대조도 실험에서는 95 mGy 에서 36 CT-번호를 구별할 수 있음을 확인하였고, 공간 해상도 실험에서는 14 lp/mm 의 성능을 확인하였다. 소 동물 촬영 결과로 실험용 쥐의 대퇴부, 심장, 그리고 복부 동맥 혈관을 촬영한 영상을 제시하였다. 개발된 micro-CT 시스템은 소 동물을 이용한 생명공학 분야 연구에 널리 이용될 수 있을 것으로 기대된다.

Abstract : We developed an x-ray cone-beam micro computed tomography (micro-CT) system for small-animal imaging. The micro-CT system consists of a 2-D flat-panel x-ray detector with a field-of-view (FOV) of 120×120 mm2, a micro-focus x-ray source, a scan controller and a parallel image reconstruction system. Imaging performances of the micro-CT system have been evaluated in terms of contrast and spatial resolution. The minimum resolvable contrast has been found to be less than 36 CT numbers at the dose of 95 mGy and the spatial resolution about 14 lp/mm. As small animal imaging results, we present high resolution 3-D images of rat organs including a femur, a heart and vessels. We expected that the developed micro-CT system can be greatly used in biomedical studies using small animals.
Key words : Micro tomography, Small animal imaging, Flat panel detector, Performance evaluation, 3D reconstruction

INTRODUCTION

Recently, there have been rapid developments in small-animal imaging technology to screen genetically engineered small animals in developing new drugs or new diagnosis/therapy methods[1-3]. Among the newly developed small-animal imaging modalities, micro-CT is believed to be very potential for accurate measurement of organ anatomy in a minimally invasive way[4-6]. It is of paramount importance in genomics to screen genetically engineered small animals in a minimally invasive way since longitudinal studies through the lifetime of the small animals are essential in the investigation of new drug/therapy effect with human disease models[7-8]. Although micro-CTs have inherent limitation in signal-to-noise ratio (SNR) performance due to their small voxel size and low x-ray exposure level, a micro-CT can be effectively used to scan bony structures or contrast agent containing vessels of a small animal.

In early micro-CT systems, x-ray image intensifiers (XRIIs) were frequently used for x-ray detection[9]. A cooled CCD coupled to a scintillating plate via an optical taper is now known to be the most sensitive one among the currently available x-ray detection methods[10]. However, it is very difficult to make a large-area detector using the cooled CCD technology aside from its high cost. To image a small animal as big as a laboratory rat, we have used a flat-panel detector with the size of 120 ×120mm2. In this paper, we describe the developmentof a micro-CT system and the evaluation of its imaging performance in terms of contrast-to-noise behavior and spatial resolution. In addition, some postmortem laboratory ratimaging and extracted rat organ imaging results are presented.

This work supported by a grant of KISTEP, Republic of Korea (M2-0305-04-0005)
통신저자 : Soo Yeol Lee, 1 Seochun, Kiheung, Yongin, Kyungki 449-701, South Korea
Graduate School of East-West Medical Science, Kyung Hee University
Tel : +82-31-201-2980, Fax : +82-31-201-3666
E-mail : sylee01@khu.ac.kr

Micro-CT system development

We show the schematic diagram of the developed micro-CT system in Fig. 1. The system consists of an x-ray source, an x-ray detector, a sample holder, a scan controller and image reconstruction processors.

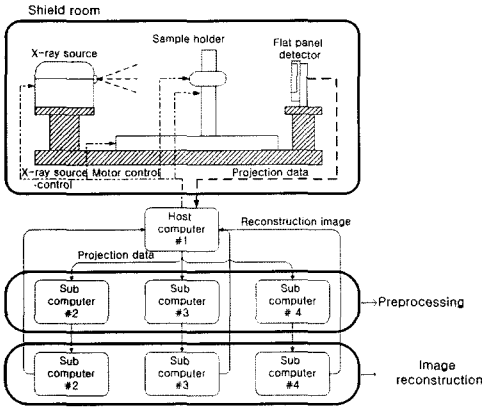

Fig. 1. Schematic diagram of the developed micro-CT system

1. X-ray source and detector

The micro-focus x-ray source (L8121-01, Hamamatsu, Japan) is a sealed tube with a fixed tungsten anode having an angle of 25against electron beam and with a 200-mm-thick beryllium exit window. The emitted x-ray beam angle is approximately 43. The source has a variable focal spot size from 5 mm to 50mm depending on the applied tube power (Watt or kVp×mA). The maximum tube voltage and tube current are 150 kVp and 500 mA, respectively.

A commercially available flat-panel detector (C7942, Hamamatsu, Japan) has been used as the 2D digital x-ray imager in the micro-CT system. The flat-panel detector consists of a 2400×2400 active matrix of transistors and photodiodes with a pixel pitch of 50 mm and a CsI:Tl scintillator. The detector has a 12bit analog-to-digital conversion and the maximum frame rate is 7Hz in the 4 ×4 binning mode. Through the measurement of modulation transfer function (MTF) based on the slant-slit method[11], it has been found that the detector has about 7 lp/mm resolving power at 10% of MTF as shown in Fig. 2. At the MTF measurement, an image of 10-mm-wide slit (I.I.E. GmbH, Aachen, Germany) slanted by 2.2to the horizontal axis was obtained with the x-ray source operating at 60 kVp and 1-mm-thick aluminum filtration. The MTF measurement results suggest that the CMOS flat-panel detector is very promising for a small-animal imaging micro-CT[12].

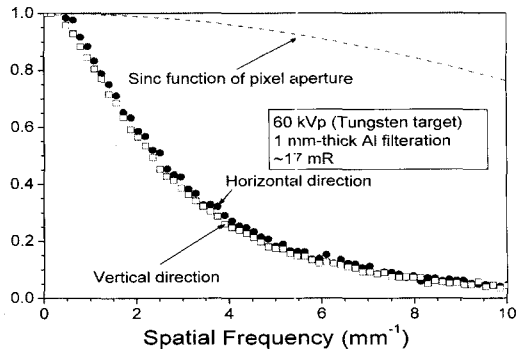

Fig. 2. DetectorMTF measurement result

2. Scan controller

It is necessary to collect cone-beam projection data with rotating the x-ray cone-beam over 360 for the scan in a cone-beam mode CT. In conventional medical CTs, the x-ray source and detector are rotated for the scan[13]. However, we rotate the sample for the scan in the developed micro-CT system to control the magnification ratio in the imaging. The sampleholder is positioned on the axis connecting the focal spot of the x-ray source and the center of the detector plane. The distance between the sample holder and the x-ray source can be adjusted according to the desired magnification ratio. The rotation is controlled by a micro stepping motor with the accuracy of 0.083. The translation of the sample holder is controlled by a stepping motor and a ball screw. We have tested the precision of the translational motion with a laser displacement sensor (Polaris70, LAP, Germany). We found that the maximum translational error is less than 5mm when the translation span is between 10mm and 100mm. The commandsignals to control the motors are transferredfrom the host computer to the motor controllers through the RS232 serial communication link (Fig. 3).

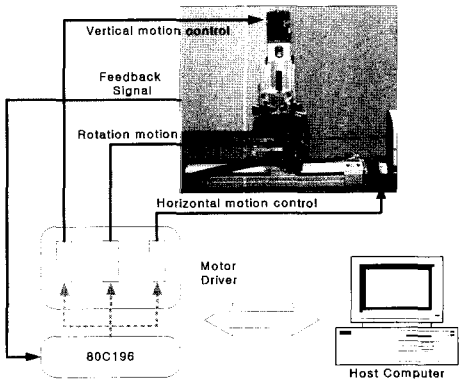

Fig. 3. The scan controller

3. Distributed image reconstruction system

Table 1. Image reconstruction time comparison (900view, 512 x 512 pixels)

	Single computer with a CPU	Single computer with dual CPUs	2 computers with dual CPUs	4 computers with dual CPUs
Reconstruction time/slice	17.3 sec	7.8 sec	3.8 sec	1.9 sec

For the cone-beam mode image reconstruction, we used the Feldkamp algorithm[14].

Since the cone-beam image reconstruction algorithm is computationallyintensive[15]and a micro-CT with a flat-panel detector makes massive projection data, it is desirable to use a parallel data processing system to speed up image reconstructions. The size of the cone-beam projection data often exceeds 13GB(2400×2400 ×1200×2 bytes) in the micro-CT. To realize a parallel data processing system, we have linked four personal computers, each one equipped with dual CPUs (Athlon MP 2200+, AMD, USA) and 2GB RAM, by 100 Mbps Ethernetand assigned evenly divided tasks to each of the eight CPUs. One of the four computers was chosen as a host computer and the host computer controls the whole micro-CT system. The host computer also acquires x-ray projection data through a frame grabber and sends the data to the other computers. The operating system of the computers is Microsoft Windows 2000 supporting dual CPUs and multi-thread processing. The projection data are sent to each computer in every four views. During the scan, each computer performs pre-processing, such as base line removal and bad pixel corrections, and projection data filtering. Each computer also performs back-projection of one fourth of the whole projection data. After back-projections are completed, the partly reconstructed images are combined to form final images in the host computer[16]. In table 1, we show the reconstruction time per slice for the various cases. As can be seen from the table, the image reconstruction time is shortened in proportion to the number of CPUs employed in the parallel data processing.

PERFORMANCE EVALUATION METHOD

1. System compensation and calibration

For precise CT image reconstruction, non-ideal properties of the components should be compensated. In this study, detector defects and misalignments of the scanning devices have been compensated. Detector defects are mostly due to non-uniformity of pixel sensitivity and bad pixels. The bad pixel compensation was performed in two steps. In the first step, we found the position of bad pixels with a 3×3 differentiation operator. If the differentiation at the given pixel was greater than the threshold value, the pixel was classified as a bad pixel. In the second step, the intensity value at the bad pixel was determined by linear interpolations of nearby pixel values. For the non-uniformity compensation, we obtained a white reference image and a dark reference image. For the reference images, we took an average of 100 images. After obtaining the reference images, each projection data was subtracted by the dark reference image and then divided by the white reference image.

Even though we used high precision rotator and translators for the CT scan, it was always necessary to calibrate the misalignments of the rotation axis and translation axis of the scanning geometry. For the calibration, we made a calibration phantom as shown in Fig. 4(a). The phantom was made of a copper plate on which holes of 15mm diameter were pierced. We took projection images of the phantom at three different positions as shown in Fig. 4(b). With the information of hole positions in the projection images, we calculated the amount of misalignments of the scanning axes and adjusted the x-ray source and detector positions and detector tilt angle with precision screws. We repeated the procedures until the amount of misalignment reached the desired value.

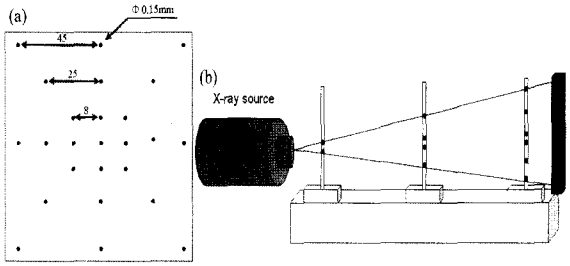

Fig. 4. (a) The phantom for misalignment calibration and (b) the phantom positioning at three different places to estimate the misalignment

2. Performance evaluation

Most measurements for the performance evaluation were performed with the x-ray source operating at 60 kVp and 1 mm Al filtration. Spatial resolution was measured in the small focal spot mode (5 m) and other performances were measured in the large focal spot mode (50 m) of the x-ray source. Typical magnification ratio was about 2. Radiation doses, addressed in the study, are based on the exposure measurement in the air at the axis of ratation with a calibrated ion chamber (Victoreen 6000-528, Inovision, USA). To take into account the dose, the measured exposure has been converted to the air kerma with the exposure-to-air kerma conversion factor 8.767 mGy/R at the x-ray spectrum of 60 kVp [17]. The frame time of the flat-panel detector to acquire a view of projection data has been kept constant at about 250 ms all over the CT scans. Typical voxel volume and image format of the reconstructed images are 100×100×200 mm3 and 512×512, respectively. For all the image reconstructions in this study, the Ram-Lak filter was used for filtering the projection data before backprojections[18].

We have tested low-contrast visibility using a contrast phantom shown in Fig. 5(a). The contrast phantom consists of six inserts whose physical densities are similar to that of water. The six inserts with 5 mm diameter were immersed in a water bath made of a 40 mm diameter acryl cylinder. The inserts were made of commercial electron density phantoms (Model 76-430, Nuclear Associates, NY, USA).

We have evaluated the spatial resolving power of the micro-CT system using the phantom shown in Fig. 5(b). The phantom is made of an 18 mm thick aluminum foil attached on an acrylic plate. The acrylic plate has a rectangular channel on which the foil is laid. The images was acquired with the voxel size of 25×25×25 mm3 and the focal spot size of 5 mm. We used the slant-slit method in calculating the MTF curve[19].

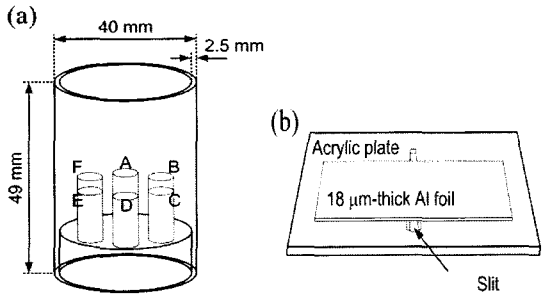

Fig. 5. The phantoms for the performance evaluation.

EXPERIMENTAL RESULTS

Fig. 6. shows a transaxial image of the contrast phantom obtained with the dose of 95mGy. We have applied narrow threshold windows to the images for clear differentiation of contrast material areas. The CT numbers of plastic water, nylon, polyethylene, acryl, polystyrene and polycarbonate are 383.2, -47.7, -203.8, -2.6, -166.6 and -35.5, respectively. We can notice that the developed micro-CT can differentiate less than 36 CT numbers at the dose of 95 mGy.

Fig. 7. shows the measured MTF of the micro-CT system at the magnification ratio of 2 as well as the detector MTF. From the results, we can notice that the system MTF is almost determined by the detector resolving power. If we assume that the limiting spatial resolution corresponds to the point when the MTF drops to 10%, then we can infer that the spatial resolution limit of the micro-CT system is about 14 lp/mm at a magnification ratio of two. It is expected that the spatial resolution of the micro-CT can reach up to 10-20 mm if we increase the magnification ratio.

For animal studies, we have obtained extracted rat organ images. Fig. 8. shows rat femur images. The femur was taken from a SD rat(age: 3months, weight: 300g). The voxel size of the images is 20×20×20 m3 and the image matrix size is 512 ×512×250. As can be noticed from the cross-sectional images, the micro-CT provides very high resolution images of the trabecular bone structures. We think that the bone structure images can be greatly used for osteoporosis studies. In Fig. 9, 3D rendered heart and vesselimages are shown. The heart image was taken with a heart organ extracted from aSD rat (age: 6months, weight: 600g), and the vessel image was taken with a sacrificed SD rat (age: 4months, weight: 500g). Prior to the heart and vessel imaging, we injected contrast agent of 2ml (omnipaque 300mgI/ml, NYCOMED) into the artery of the rat. The image voxel size is 50×50×50 m3 with the matrix size of 512×512×300.

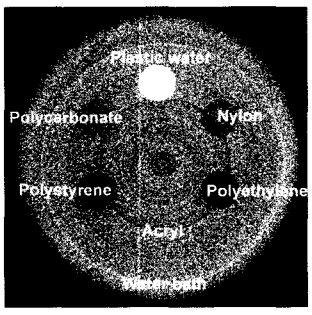

Fig. 6. The reconstructed contrast phantom image

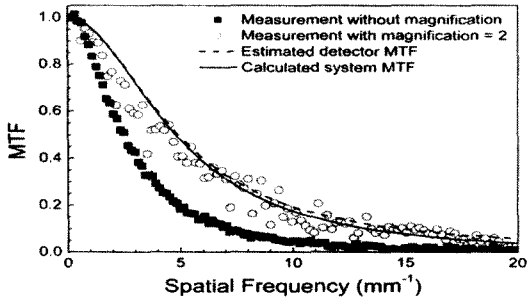

Fig. 7. MTFof the micro-CT system

Fig. 8. Rat femur images obtained with the micro-CT system.

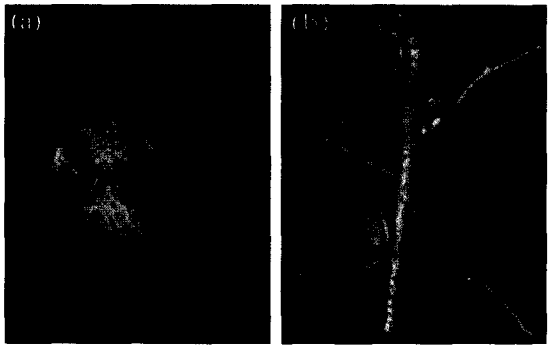

Fig. 9. 3D rendered heart and vessel images obtained with the micro-CT system.

DISCUSSIONS AND CONCLUSIONS

An indirect-detection CMOS flat panel detector has been successfully used in the prototype micro-CT developed for small-animal imaging. The advantages of the flat panel detector in a micro-CT over other type of detectors are manifold. Commercially available flat panel detectors can be readily used for whole body imaging of small animals as large as laboratory rats. Since the flat panel detector technology is fast growing by the needs of mass production, availability and low cost are other merits in a micro-CT.

In small-animal imaging with a micro-CT, long scan time to ensure soft tissue visibility seems to be most troublesome. With a micro-CT consisting of a flat panel detector, a scan time of at least several minutes is inevitable to differentiate organs in the abdomen region. Due to the long scan time, in vivo rat or mouse images suffer from cardiac and respiratory motion artifacts. To authors' knowledge, most of small animal studies reported so far have been performed on post mortem animals with a micro-CT. For the micro-CT to be useful in small-animal imaging, we think that respiratory motion artifact reduction techniques should be incorporated.

In conclusions, flat panel detectors can be used in a micro-CT aiming at small-animal imaging. If a long scan time can be accepted, the flat panel detector can give good contrast images with a spatial resolution of an order of 10-20 m.

REFERENCES

1. T. F. Massoud and S. S. Gambhir, "*Molecular imaging in living subject: seeing fundamental biological processes in a new light*", Genes & Development, 17, pp. 545-580, 2003
2. M. G. Pomper, "*Molecular imaging: an overview*",Acad. Radiol., 8, pp. 1141-1153, 2001
3. R. Weissleder and U. Mahmood, "*Molecular imaging*", Radiology, 219, pp. 316-333, 2001
4. S. M. Jorgensen, O. Demirkaya and E. L. Ritman, "*Three-dimensional imaging of vasculature and parenchyma in intact rodent organs with x-ray micro-CT*", Am. J. Physiol., 275, H1103-1114, 1998
5. M. J. Paulus, H. Sari-Sarraf, S. S. Gleason, M. Bobrek, J. S. Hicks, D. K. Johnson, J. K. Behel, L. H. Thompson and W. C. Allen, "*A new x-ray computed tomography system for laboratory mouse imaging*",IEEE. Trans. Nucl. Sci., 46, pp. 558-564, 1999
6. S. Y. Wan S Y, A. P. Kiraly, E. L. Ritman and W. E. Higgins, "*Extraction of the hepatic vasculature in rats using 3-D micro-CT images*",IEEE. Trans. Med. Imag., 19, pp. 964-971, 2000
7. M. J. Paulus, S. S. Gleason, H. Sari-Sarraf, D. K. Johnson, C. J. Foltz, D. W. Austin, M. E. Easterly, E. J. Michaud, M. S. Dhar, P. R. Hunsicker, J. W. Wall and M. Schell, "*High-resolution x-ray CT screening of mutant mouse models*", Proc. SPIE, 3921, pp. 270-279, 2000
8. E. L. Ritman, "*Molecular imaging in small animals-roles for micro-CT*", J. Cell. Biochem. Supp., 39, pp. 116-124, 2002
9. D. W. Holdsworth, M. Drangova and A. Fenster, "*A high-resolution XRII-based quantitative volume CT scanner*", Med. Phys., 20, pp. 449-462, 1993
10. G. Wang and M. Vannier, "*Micro-CT scanners for biomedical applications: an overview*", Advanced Imaging,

16, pp. 18-27, 2001
11. H. Fujita, D. Y. Tsai, T. Itoh, K. Doi, J. Morishita, K. Ueda and A. Ohtsuka, "*A simple method for determining the modulation transfer function in digital radiography*", IEEE. Trans. Med. Imag., 11, pp. 34-39, 1992
12. S. C. Lee, H. K. Kim, I. K. Chun, M. H. Cho, S. Y. Lee and M. H. Cho, "*A flat-panel detector based micro-CT system: performance evaluation for small-animal imaging*", Phys. Med. Biol., 48, pp. 4173-4185, 2003
13. S. C. Lee, M. H. Cho and S. Y. Lee, "*Performance comparison of reconstruction algorithms for fan-beam computerized tomography*", J. Biomed. Eng. Res., 22, pp. 223-229, 2001
14. L. A. Feldkamp, L. C. Davis and J. W. Kress, "*Practical cone-beam algorithm*", J. Opt. Soc. Am. A, 1, pp. 612-619, 1984
15. C. A. Carlsson, "*Imaging modality in x-ray computerized tomography and in selected volume tomography*", Phys. Med. Biol., 44, R23-56, 1999
16. S. C. Lee, J. Y. Han, I. K. Chun, S. Y. Lee and M. H. Cho, "*Distributed image reconstruction for an in-vivo mouse imaging system*", Proc. SPIE, 5030, pp. 639-646, 2003
17. J. M. Boone, Handbook of Medical Imaging, Bellingham: SPIE Press, pp. 1-78, 2000
18. G. N. Ramachandran and A. V. Lakshminarayanan, "*Three dimensional reconstructions from radiographs and electron micrographs: application of convolution instead of Fourier transforms*", Proc. Natl. Acad. Sci., 68, pp. 2236-2240, 1971
19. J. M. Boone, "*Determination of the presampled MTF in computed tomography*", Med. Phys., 28, pp. 356-360, 2001